Catalysis Letters, Vol. 116, Nos. 3–4, August 2007 (© 2007)
DOI: 10.1007/s10562-007-9144-3

Rational design of gold catalysts with enhanced thermal stability: post modification of Au/TiO_2 by amorphous SiO_2 decoration

Haoguo Zhu, Zhen Ma, Steven H. Overbury, and Sheng Dai

Chemical Sciences Division and Center for Nanophase Materials Sciences, Oak Ridge National Laboratory, Oak Ridge, TN 37831, USA

Received 15 April 2007; accepted 15 May 2007

Au/TiO_2 is highly active for CO oxidation, but it often suffers from sintering in high-temperature environments. In this work, we report on a novel design of gold catalysts, in which pre-formed Au/TiO_2 catalysts were post decorated by amorphous SiO_2 to suppress the agglomeration of gold particles. Even after being aged in O_2–He at 700 °C, the SiO_2-decorated Au/TiO_2 was still active for CO oxidation at ambient temperature.

KEY WORDS: gold nanoparticles; CO oxidation; promotion; sintering; alkoxysilanes; post decoration.

1. Introduction

One of the driving forces of contemporary catalysis research is the rational design of novel catalytic materials [1,2]. In rational design, one first identifies the key functions to be actualized and then advertently synthesizes catalytic materials according to the desired functions [3–5]. In the specific case of catalysis by supported gold nanoparticles, two functionalities, namely, the catalytic activity and thermal stability of catalysts, are particularly important. It is known that Au/SiO_2 usually exhibits very low activity in CO oxidation. On the other hand, Au/TiO_2 is highly active for CO oxidation, but it suffers from significant loss of activity upon high-temperature calcination [6–10]. The latter situation may adversely influence the practical applications of Au/TiO_2 when the operation and regeneration of catalysts at elevated temperature are needed [11,12].

To improve the activity of SiO_2-based gold catalysts, our group has modified mesoporous [13] or fumed [14] SiO_2 supports with TiO_2 coatings via a surface-sol-gel method, and then loaded gold. The idea is to increase the isoelectric point of the support and to control the local structure of active centers through surface functionalization so as to facilitate the deposition of gold and to enhance the catalytic activity. Other researchers have modified SiO_2 supports by TiO_2 [15,16] or CoO_x [17–19] for loading gold. Alternatively, we used $Au(en)_2Cl_3$ instead of $HAuCl_4$ as the precursor, and succeeded in the preparation of highly active Au/SiO_2 catalysts through deposition of the above gold precursor under basic conditions [20,21]. Other researchers have also successfully prepared active Au/SiO_2 with different designs [22–25].

To improve the thermal stability of Au/TiO_2, we coated TiO_2 with a thin layer of Al_2O_3 via a surface-sol-gel method, and then loaded gold nanoparticles [26]. The maintenance of activity in CO oxidation after calcination at 500 °C was ascribed to the stabilization of gold particles against agglomeration [26]. Others have loaded gold particles on MgO- or BaO-modified Al_2O_3, and found similar stabilization effects [27,28]. Recently, we demonstrated that the surface-sol-gel method [26] is not necessary because conventional impregnation using $Al(NO_3)_3$ precursor followed by thermal decomposition to form dispersed Al_2O_3 on TiO_2 worked well, and that Al_2O_3 additive [26] is not unique because other selected metal oxide additives exhibited comparable or even better stabilizing effects [29].

In this work, we report on a rational design of Au/TiO_2-based catalysts with enhanced thermal stability through post modification of Au/TiO_2 by amorphous SiO_2 decoration (figure 1). This design is essentially different from the conventional one in which surface-modified oxide supports were prepared first, and then gold was loaded [13–16,26–29]. The current post-decoration design is based on the rationale that the pre-formed gold-TiO_2 interface may provide high activity for CO oxidation [6–10], whereas the subsequently loaded SiO_2 decoration may serve as a textural promoter to mitigate the agglomeration of gold nanoparticles.

2. Experimental

Au/TiO_2 was prepared by deposition-precipitation [6–10]. First, 150 mL aqueous $HAuCl_4$ solution

*To whom correspondence should be addressed.
E-mail: dais@ornl.gov

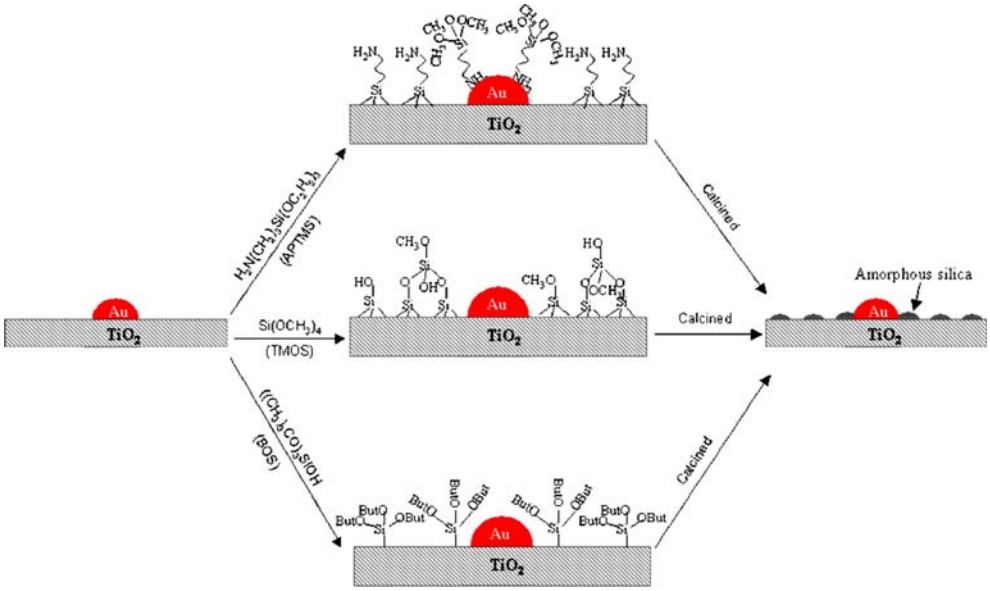

Figure 1. Proposed scheme for the synthesis of SiO_2-decorated Au/TiO_2. Pre-formed Au/TiO_2 was treated in tetramethyl orthosilane (TMOS, $Si(OCH_3)_4$), (3-aminopropyl)trimethoxysilane (APTMS, $H_2N(CH_2)_3Si(OC_2H_5)_3$), or tris(*tert*-butoxy)silanol (BOS, $((CH_3)_3CO)_3SiOH$) solution, followed by calcination.

containing 0.9 g $HAuCl_4{\cdot}3H_2O$ was titrated by 5.0 wt% NaOH to pH 10, and mixed with 4.0 g TiO_2 (Degussa P25, surface area 48 m^2/g) under vigorous stirring. The suspension was subsequently re-titrated to pH 10, and stirred at 70 °C for 2 h. The precipitate was centrifuged, thoroughly washed with water, dried in a vacuum oven at 60 °C overnight, and calcined in a muffle oven at 300 °C for 3 h.

To synthesize SiO_2-decorated Au/TiO_2 (denoted as $SiO_2/Au/TiO_2$), 0.5 g Au/TiO_2 (which was calcined in a muffle oven at 300 °C for 3 h, as described above) was dispersed in 100 mL ethanol, 3.4 g tetramethyl orthosilane (TMOS, $Si(OCH_3)_4$), or 1.0 g (3-aminopropyl)trimethoxysilane (APTMS, $H_2N(CH_2)_3Si(OC_2H_5)_3$), or 0.5 g tris(*tert*-butoxy)silanol (BOS, $((CH_3)_3CO)_3SiOH$) added, and the suspension stirred at room temperature for 5–15 h under N_2 atmosphere. The product was centrifuged and dried in a vacuum oven at 60 °C.

To synthesize gold supported on SiO_2-decorated TiO_2 (denoted as $Au/SiO_2/TiO_2$) for a control experiment, 1.0 g TiO_2 was dispersed in 200 mL ethanol, 6.8 g tetramethyl orthosilane added, and the suspension stirred at room temperature for 15 h. The resulting material was centrifuged, dried in vacuum, and calcined in a muffle oven at 500 °C for 2 h. Gold was loaded via deposition-precipitation according to the procedure described in the above paragraph, and the resulting sample was calcined in a muffle oven at 300 °C for 3 h.

To perform reaction testing, 50 mg catalyst was packed into a U-shaped silica tube (4 mm i.d.), and was calcined under flowing 8% O_2–He at 500 or 700°C for 1–5 h (heating rate: 30 °C/min) on an AMI 200 microreactor. CO oxidation was performed by flowing 1% CO (balance air, <4 ppm H_2O) through the catalyst at a rate of 37 cm^3/min, and the reaction temperature was varied using a furnace or by immersing the U-type tube in ice-water or acetone-liquid N_2. The reaction mixture was analyzed by a dual-column GC with a thermal conductivity detector.

To characterize the catalysts, XRD data were collected on a Siemens D5005 diffractometer with Cu K_α radiation. The average gold particle sizes were estimated from X-ray line broadening analysis applying the Debye-Scherrer equation on the (220) diffraction (2θ = 44 °) of gold. The gold content was analyzed using inductivity coupled plasma-optical emission spectrometry on a Thermo IRIS Intrepid II spectrometer. The Si/Ti molar ratio was estimated by EDAX on a JOEL JSM-6060 scanning electron microscope coupled with an EDAX detector. TGA/DTG experiments were conducted on a TGA 2950 instrument using a heating rate of 10 °C/min under air atmosphere. TEM experiments were performed using a Hitachi HD-2000 STEM operating at 200 kV.

3. Results and discussion

3.1. Au/TiO_2: activity and thermal sintering

Figure 2A shows the light-off curves of Au/TiO_2. Au/TiO_2, calcined in a muffle oven at 300 °C according to the temperature used by Haruta *et al.* [6], was very active for CO oxidation, achieving T_{50} (temperature required for 50% conversion) value of −37 °C. However, its catalytic activity significantly decreased upon further calcination at higher temperatures in flowing O_2–He. The T_{50} values increased to 30, 84, and 127 °C when Au/TiO_2 was calcined at 500 °C for 1, 3, and 5 h,

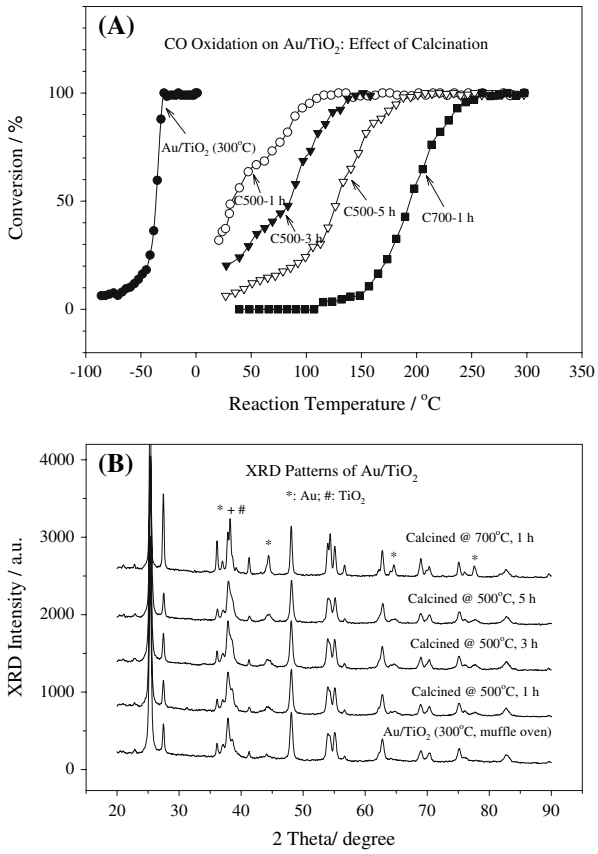

Figure 2. CO light-off curves (A) and XRD patterns (B) of Au/TiO_2 calcined in a muffle oven at 300 °C and Au/TiO_2 further calcined in O_2–He at 500 °C for 1–5 h or at 700 °C for 1 h.

respectively, and further increased to 196 °C when Au/TiO_2 was calcined at 700 °C for 1 h, indicating severe thermal deactivation commonly seen in the literature [26,29–31].

Figure 2B compares the XRD patterns of Au/TiO_2 after different treatments. In general, gold peaks appeared at $2\theta = 38$, 44, 65, and 78 °, corresponding to Au (111), (200), (220), and (311), respectively [31]. Other peaks are ascribed to those from anatase and rutile, characteristic of Degussa P25 [32]. The gold peaks became sharper with the increases in the duration and temperature of calcination, implying the growth of gold particles. The average gold particle size of Au/TiO_2 (300 °C) was estimated as 4.0 nm according to X-ray line broadening analysis. The value increased to 6.2, 7.5, and 9.5 nm after Au/TiO_2 was calcined at 500 °C for 1, 3, and 5 h, and increased to 16.5 nm after it was calcined at 700 °C for 1 h (table 1), meaning severe agglomeration of gold particles. The increase in gold particle size (table 1) is consistent with the decrease in catalytic activity (figure 2A).

In principle, metal nanoparticles have extra surface free energy and higher chemical potential than those of the bulk metal, so that they can be highly mobile even below the melting point of the bulk metal [10]. In fact, the melting point of gold nanoparticles decreases with the particle size, and is much lower than that of the bulk gold [33]. The sintering problem of gold nanaparticles is particularly acute if they are placed in O_2 atmosphere as compared to vacuum [34,35]. Because the optimal size of gold particles on TiO_2 for CO oxidation is 3–5 nm and the activity decreased greatly when the gold particle become too big [6–10,36], the agglomeration of gold particles upon high-temperature calcination is the reason that may cause catalyst deactivation.

3.2. $SiO_2(TMOS)/Au/TiO_2$: activity and thermal sintering

To mitigate the sintering of gold nanoparticles, we modified the pre-formed Au/TiO_2 by SiO_2 adlayers via chemical grafting (figure 1). Figure 3A shows the CO light-off curves on SiO_2-decorated Au/TiO_2 prepared using $Si(OCH_3)_4$ (TMOS) [37,38] as the precursor. It should be mentioned that the as-synthesized SiO_2(TMOS)/Au/TiO_2 was not very active for CO oxidation, achieving T_{50} at 239 °C, in sharp contrast to the −37 °C value obtained with Au/TiO_2 calcined at 300 °C, even though as-synthesized and 300 °C-calcined samples had similar gold particle sizes (table 1). The ineffectiveness of the as-synthesized sample may be due to the presence of unburned organic fragments, as implied from our TG/DTG experiments (figure 4). Other researchers have found that gold catalysts containing certain organic ligands or fragments are not active unless these are removed through proper pretreatment [25,31,39–45].

Once the SiO_2 precursor was sufficiently decomposed and SiO_2 formed, the sample exhibited improved thermal stability. The T_{50} values of SiO_2(TMOS)/Au/TiO_2 were 27, 50, and 57 °C when the sample was calcined in O_2–He at 500 °C for 1, 3, and 5 h, respectively. The T_{50} value was maintained at 64 °C when SiO_2(TMOS)/Au/TiO_2 was subject to calcination at 700 °C (figure 3 and table 1). Recall that the T_{50} of unmodified Au/TiO_2 was as large as 196 °C after aging at 700 °C (figure 2 and table 1). Thus, the stabilizing effect of the SiO_2 adlayer is obvious.

Figure 3B shows the XRD patterns of SiO_2-decorated Au/TiO_2 after different treatments. The gold peaks were all broad, and no drastic sharpening of the gold peaks was seen after thermal treatments. In particular, the average gold particle size of SiO_2(TMOS)/Au/TiO_2 was estimated as 6.5 nm after 700 °C-calcination, much smaller than the 16.5 nm value with unmodified Au/TiO_2 after 700 °C-calcination (table 1). Preliminary TEM data indicated that 700 °C-calcined SiO_2(TMOS)/Au/TiO_2 mainly contained gold particles with sizes of 3–15 nm, and 700 °C-calcined Au/TiO_2 mainly contained gold particles with sizes of 10–50 nm (data not shown). These data further confirm the stabilizing effect of the amorphous SiO_2 modifier.

Another noticeable trend in figure 3B is that the relative intensities of TiO_2 peaks were not significantly

Table 1
Gold loadings (measured by ICP), Si/Ti ratios (by EDAX), average gold particle sizes (by XRD), and T_{50} values of Au/TiO_2, $SiO_2/Au/TiO_2$, and $Au/SiO_2/TiO_2$ samples

Sample	Au loading, wt%	Si/Ti molar ratio	Average gold particle size [a], nm	T_{50}, °C
Au/TiO_2 (300 °C, muffle oven)	3.3		4.0	−37
Au/TiO_2-C500-1 h			6.2	30
Au/TiO_2-C500-3 h			7.5	84
Au/TiO_2-C500-5 h			9.5	127
Au/TiO_2-C700-1 h			16.5	196
As-synthesized SiO_2(TMOS)/Au/TiO_2			4.5[b]	239
SiO_2(TMOS)/Au/TiO_2-C500-1 h	2.2	0.10	5.3	27
SiO_2(TMOS)/Au/TiO_2-C500-3 h			5.5	50
SiO_2(TMOS)/Au/TiO_2-C500-5 h			6.0	57
SiO_2(TMOS)/Au/TiO_2-C700-1 h			6.5	64
As-synthesized SiO_2(APTMS)/Au/TiO_2			4.7[b]	228
SiO_2(APTMS)/Au/TiO_2-C500-1 h	2.5	0.06	5.4	26
SiO_2(APTMS)/Au/TiO_2-C500-3 h			5.7	30
SiO_2(APTMS)/Au/TiO_2-C500-5 h			6.2	29
SiO_2(APTMS)/Au/TiO_2-C700-1 h			7.1	85
As-synthesized SiO_2(BOS)/Au/TiO_2			4.7[b]	141
SiO_2(BOS)/Au/TiO_2-C500-1 h	2.5	0.004	5.3	15
SiO_2(BOS)/Au/TiO_2-C500-3 h			5.9	40
SiO_2(BOS)/Au/TiO_2-C500-5 h			7.0	69
SiO_2(BOS)/Au/TiO_2-C700-1 h			12.0	110
Au/SiO_2(TMOS)/TiO_2 (300 °C, muffle oven)			b, c	160
Au/SiO_2(TMOS)/TiO_2-C700-1 h	0.1	0.11	c	> 520

[a] measured after reaction testing unless otherwise indicated.
[b] measured before reaction testing.
[c] gold peaks were not clearly detected by XRD because of low gold loading.

changed. This is in contrast to the case shown in figure 2B, in which the peaks corresponding to the rutile phase (2θ = 27, 36, 41, and 54 °) obviously intensified after calcining Au/TiO_2 at 700 °C. By comparing both figures 2B and 3B, it is clear that the post-decoration of Au/TiO_2 by SiO_2 not only suppressed the growth of gold, but also suppressed the transformation of anatase to rutile. It is well known in the literature that the dispersion of sulfate, like that of SiO_2 in the current case, can retard the phase transformation of TiO_2 [46]. It is also expected that certain structural changes of the supports during calcination may bring detrimental effects to the stabilization of gold particles [10].

Although the effects of SiO_2 on catalytic activity and structure of the catalyst are obvious (figure 3), no crystalline SiO_2 peaks were detected by XRD in figure 3B. This could be potentially interpreted as either the SiO_2 species was amorphous, or the uptake of SiO_2 was negligible. However, Si element was clearly detected in EDAX experiments (figure 5), and the Si/Ti molar ratio was estimated as 0.1, thus confirming that SiO_2 was loaded. In fact, it is well established that alkoxysilanes can condense with hydroxyl groups on metal oxide surfaces [37,38].

3.3. Effect of other SiO_2 precursors

To test whether the methodology of decorating Au/TiO_2 by amorphous SiO_2 is general, other SiO_2 precursors, such as $H_2N(CH_2)_3Si(OC_2H_5)_3$ (APTMS) [47] and $((CH_3)_3CO)_3SiOH$ (BOS) [48] were preliminarily tried. The amine group of APTMS is known to interact with gold surfaces [49], and the OC_2H_5 groups can also condense with the surface hydroxyl groups [47]. This amine-gold interaction may provide a driving force to enrich APTMS in the close vicinity of gold nanoparticles, thereby controlling the spatial location of the surface decoration of SiO_2 (figure 1). On the other hand, the rationale behind the use of BOS is to investigate the use of the stereochemistry of siloxane precursors in controlling the surface decoration density of SiO_2 (figure 1). As seen from table 1, the Si content of SiO_2(APTMS)/Au/TiO_2 (Si/Ti $\sim$ 0.06) is only a little lower than that of SiO_2(TMOS)/Au/TiO_2 (Si/Ti $\sim$ 0.1), while the Si content of SiO_2/(BOS)/Au/TiO_2 (Si/Ti $\sim$ 0.004) is the lowest. The low Si content of SiO_2/(BOS)/Au/TiO_2 could be attributed to the fact that BOS is bulkier than TMOS, thus resulting in the low surface functonalization efficiency of BOS (figure 1). Alternatively, one could also argue that this may be due to the fact that the amount of BOS (0.5 g, equivalent to 0.002 mol) put in the synthesis mixture was less than that of TMOS (3.4 g, equivalent to 0.02 mol). However, preliminary data obtained by our group indicated that when the chemical grafting was carried out room temperature, as the grafting temperature used here, even using much more BOS, the Si/Ti ratio was still comparably low [50].

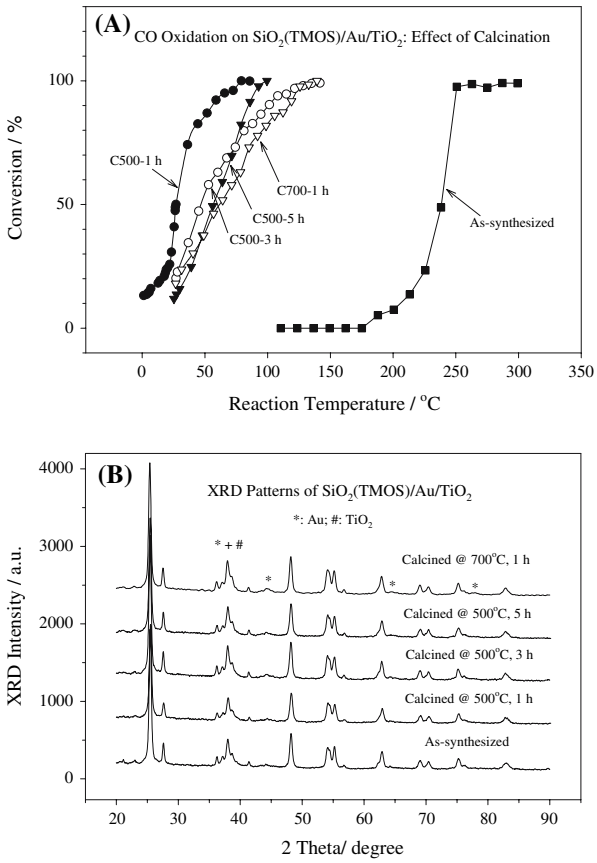

Figure 3. CO light-off curves (figure 3A) and XRD patterns (figure 3B) of as-synthesized SiO_2(TMOS)/Au/TiO_2 and those further calcined in O_2–He at 500 °C for 1–5 h or at 700 °C for 1 h.

The as-synthesized SiO_2(APTMS)/Au/TiO_2 and SiO_2(BOS)/Au/TiO_2 were again not very active, achieving 50% CO conversion at 228 and 141 °C, respectively (table 1). This is again due to the presence of residual organic fragments, as verified from TG/DTG experiments similar to the one in figure 4 (data not shown). The residual organic fragments do not have to be completely removed to actualize some activity,

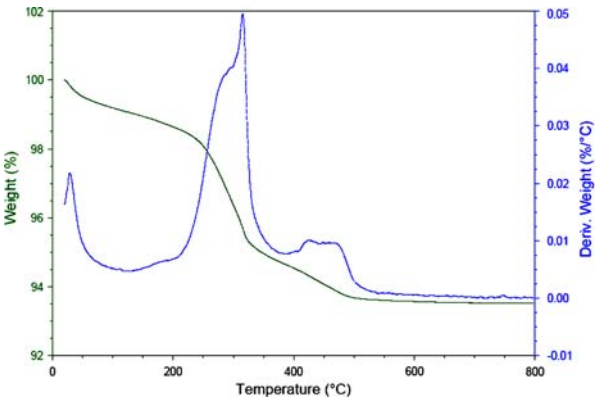

Figure 4. TG/DTG data of SiO_2(TMOS)/Au/TiO_2. The experiment, starting from as-synthesized SiO_2(TMOS)/Au/TiO_2, was conducted with a heating rate of 10 °C/min in air.

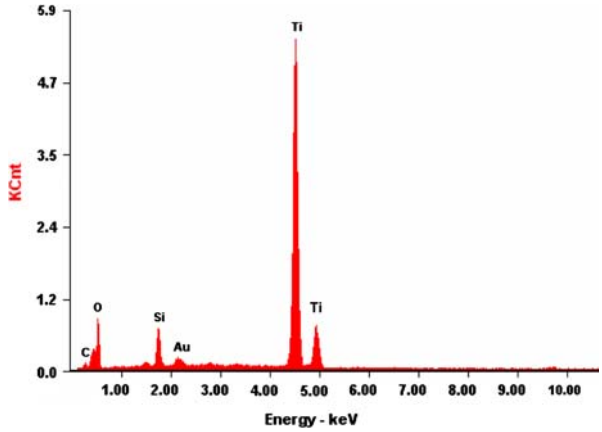

Figure 5. EDAX data of SiO_2(TMOS)/Au/TiO_2 which was calcined in O_2–He at 500 °C.

because the overall activity is expected to depend on the coverage of surface fragments and the population of the uncovered gold particles. This is the reason why as-synthesized SiO_2(BOS)/Au/TiO_2 with the lowest Si content could show some activity at relatively low temperatures (T_{50} = 141 °C). Once the organic fragments were more sufficiently removed, the resulting catalysts exhibited improved thermal stability of gold particles, thus maintaining low T_{50} values to some extent (table 1). Figure 6 shows the catalytic data of SiO_2(APTMS)/Au/TiO_2 and SiO_2(BOS)/Au/TiO_2. The sintering-resistant capability of SiO_2(APTMS)/Au/TiO_2 is similar to that of SiO_2(TMOS)/Au/TiO_2 even though the Si content of the former is less than that of the latter. This could be attributed to the selective location of SiO_2 through the interaction of amine groups with gold nanoparticles in the former catalyst system. The sintering-resistant ability of SiO_2(BOS)/Au/TiO_2 is weaker than that of SiO_2(TMOS)/Au/TiO_2, in line with the lower surface decoration density of SiO_2 in the former case (Table 1).

3.4. *Stability and regeneration of SiO_2/Au/TiO_2*

The temporal stability seen on SiO_2/Au/TiO_2 is acceptable, as demonstrated in figure 7. In this experiment, the reaction temperature was properly chosen to achieve an initial conversion below 100%, in order to clarify the stability on stream [10,51]. As shown in figure 7, the CO conversion on 500 °C-calcined SiO_2(TMOS)/Au/TiO_2 at 54 °C decreased from ca. 92 to 81% during the initial 6 h, and then gradually reached a steady-state value of ca. 70% in the following 18 h. In other experiments, the stability of 500 °C-calcined SiO_2(APTMS)/Au/SiO_2 and SiO_2(BOS)/Au/SiO_2 was found to be acceptable as well. For example, the initial CO conversion on 500 °C-calcined SiO_2(BOS)/Au/TiO_2 at 53 °C was 97%, and the steady-state conversion was 89% when the reaction time was 24 h.

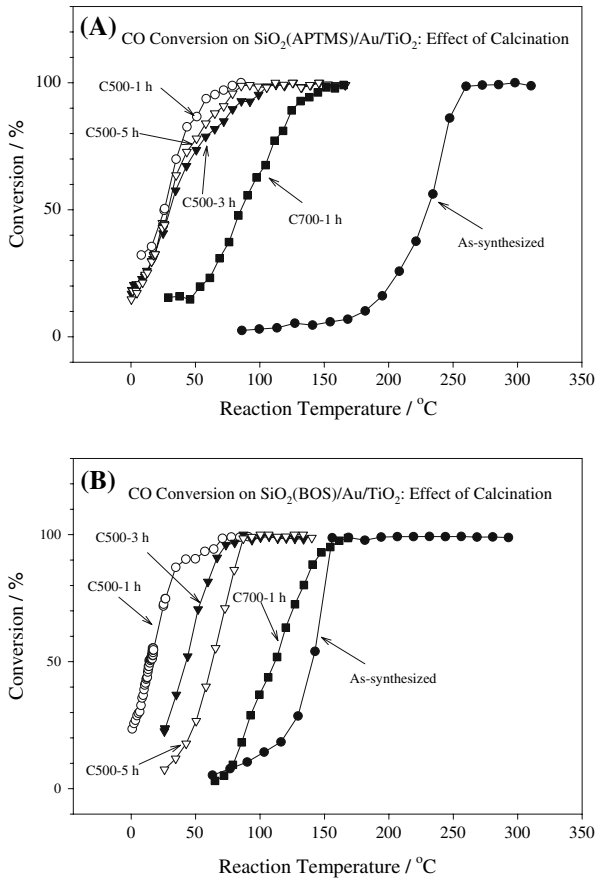

Figure 6. Panel A: CO light-off curves of as-synthesized SiO_2(APTMS)/Au/TiO_2 and those further calcined in O_2–He at 500 °C for 1–5 h or at 700 °C for 1 h. Panel B: CO light-off curves of as-synthesized SiO_2(BOS)/Au/TiO_2 and those further calcined in O_2–He at 500 °C for 1–5 h or at 700 °C for 1 h.

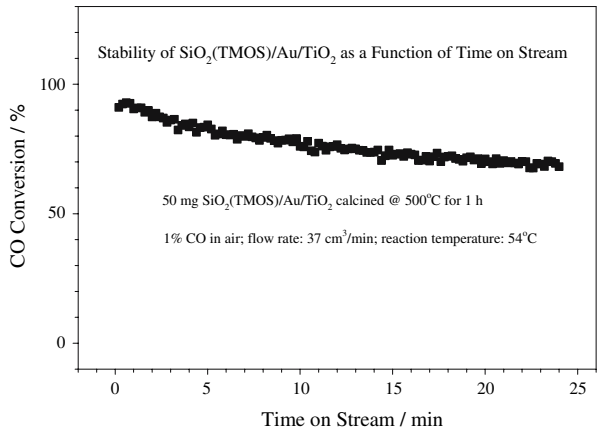

Figure 7. CO conversion on 500 °C-calcined SiO_2(TMOS)/Au/TiO_2 as a function of reaction time.

The used catalyst can be regenerated. In a preliminary regeneration experiment, the used 500 °C-calcined SiO_2(TMOS)/Au/TiO_2 catalyst, which had been stored for weeks in the U-type tube at ambient temperature after the stability test in figure 7, was treated in flowing O_2–He at 400 °C for 1 h, and then cooled down to the reaction temperature. The initial conversion at 54 °C was still 91%, comparable to the 92% value achieved on the fresh catalyst. Thus, the deactivation of SiO_2/Au/TiO_2 is not irreversible. The fact that the catalyst can be regenerated by calcination means that the catalyst deactivation is not due to the growth of gold particle sizes (because the deactivation caused by the growth of gold particle sizes is irreversible), but is likely due to the adsorption of surface intermediates such as carbonate [52]. Further research is in progress in our group to better understand the deactivation mechanism and regeneration methods.

3.5. *Control experiments: comparison of SiO_2/Au/TiO_2 and Au/SiO_2/TiO_2*

Note that the current post-decoration design is different from the conventional one in which a support (e.g., SiO_2) is modified by another metal oxide (e.g., TiO_2), and gold was subsequently loaded onto the modified support (e.g., TiO_2/SiO_2) [13,14]. The success in the deposition of gold onto TiO_2/SiO_2 in the previous design lies in the fact that neat SiO_2 is not suitable for deposition-precipitation of gold using $HAuCl_4$ precursor [6–10], because of the mismatch between the isoelectric point of SiO_2 (IEP $\sim$ 2) and the pH range needed to sufficiently hydrolyze the $HAuCl_4$ precursor to $Au(OH)_3$ or $Au(OH)_4^-$ (pH = 8–10) [10,13]. Therefore, the modification of low-IEP SiO_2 support with TiO_2 layer makes the resulting support more suitable for loading gold [13,14]. However, in the present case, if we modify the TiO_2 support with SiO_2, and then load gold, the resulting SiO_2/TiO_2 support is supposed to be less suitable for loading gold. Note that in a previous publication, the isoelectric point of TiO_2 was found to decrease from 6 to 2 after doping SiO_2 layer onto it [37]. Indeed, in control experiments, we found that the loading of gold onto such SiO_2(TMOS)/TiO_2 support led to poor catalytic performance (T_{50} = 160 and > 520 °C flowing heat treatment at 300 or 700 °C, respectively, figure 8). The reason is that gold was not effectively loaded onto SiO_2/TiO_2, as proven by the failure in detecting gold peaks by XRD (data not shown) and the low gold content as measured by ICP (0.1 wt%, table 1).

The results from our control experiment clearly indicate that the deposition-precipitation of gold is ineffective if the pre-formed SiO_2/TiO_2 support is used to load gold. However, the deposition-precipitation will not be influenced if the decoration of SiO_2 component is executed afterwards. The resulting SiO_2/Au/TiO_2 catalyst combines both the high activity of Au-TiO_2 interface [6–10] and the high thermal stability of SiO_2 component. The role of SiO_2 is expected to be a textural promoter since the gold particle sizes are stabilized by the addition of SiO_2 (table 1).

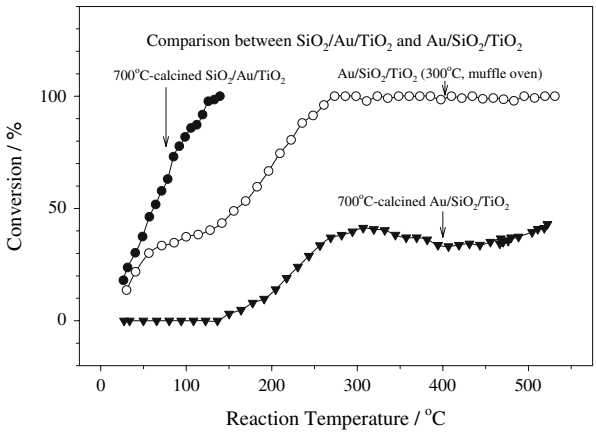

Figure 8. Comparison between the catalytic performance of SiO_2/Au/TiO_2 and Au/SiO_2/TiO_2. In the first case, pre-formed Au/TiO_2 was subsequently modified by SiO_2 matrix (see also figure 3A). In the second situation for comparison, TiO_2 was modified by SiO_2 first, and then gold was loaded onto SiO_2/TiO_2.

3.6. Discussion and perspective in the context of the literature

To the best of our knowledge, this is the first report that post-decoration of active Au/TiO_2 by inert SiO_2 could mitigate the sintering of gold nanoparticles. We are aware of the work by Horváth *et al.* who post decorated inactive Au/SiO_2 with active TiO_2 patches to create new gold-TiO_2 boundaries, thus increasing the catalytic activity for CO oxidation [53]. Analogously, Guczi *et al.* post deposited active FeO_x layers onto Au/SiO_2/Si(100) by pulsed laser deposition, and found that the activity of the FeO_x/Au/SiO_2/Si(100) model catalyst was higher than those of Au/SiO_2/Si(100) and FeO_x/SiO_2/Si(100) because of the creation of gold-FeO_x interface [54]. Others and us have post modified Au/TiO_2 by nitrate [55], sulfate [56], and phosphate [57] to study the anion effects on activity. Lu and coworkers very recently reported that the impregnation of Au/C with KNO_3 could stabilize gold particles for selective CO oxidation in hydrogen-rich gas [58]. Going beyond the supported gold system, a recent communication by Kanazawa at Toyota Motor Corporation reported that the sintering of Pt particles on MFI zeolite was suppressed after impregnating Pt/MFI with tetramethyl orthosilane, and the resulting Pt catalyst could withstand thermal aging at 1000 °C [59]. Hence, it is expected that this post-decorating method may be extended to other supported metal systems for practical or commercial applications. However, due to the limited database, it is not clear whether other oxides can also stabilize metal particles.

Note that the chemical grafting method used in the current work is essentially solution-based [12,13,15,16,26]. We have chosen room temperature as the grafting temperature because our preliminary experiments indicated certain agglomeration of gold particles during chemical grafting in the presence of very hot organic solutions containing the SiO_2 precursor (data not shown). 300 °C-calcined Au/TiO_2 was used instead of as-synthesized Au/TiO_2 for chemical grafting, due to the concern that supported Au^{3+} may react with the ethanol solvent to form at least a proportion of big gold particles [29]. Further research opportunity may open up if gas-phase atomic layer deposition [60] is used instead of the solution-phase approach to post decorate metal catalysts. Nevertheless, there could be some issues related to the low vapor pressure, low reactivity, and limited availability of certain precursors, possible inhomogeneous coatings on power samples as opposed to flat substrates, as well as the influence of residual chloride (e.g., when using $TiCl_4$ as the precursor) on catalytic activity. In addition, one has to demonstrate the advantages of gas-phase atomic layer deposition over solution-based chemical grafting or conventional impregnation if the atomic-layer-decomposition method is to be highlighted. All of these are barely addressed in the conventional preparation of supported metal catalysts [61]. In addition, considering the fact that chemical grafting is able to be carried out in ultrahigh vacuum chambers [62,63], the post-decorating design may be extended to the construction and surface-science studies of a variety of model supported catalysts to be explored in the future [54].

4. Conclusions

In this work, we have developed a novel method to improve the thermal stability of gold catalysts. In this method, pre-formed Au/TiO_2 catalyst was decorated by amorphous SiO_2 matrix using tetramethyl orthosilane, (3-aminopropyl)trimethoxysilane, or tris(*tert*-butoxy)silanol as the precursor via a solution-based approach. Both the gold particle size and the activity in CO oxidation could be maintained to some extent even after several thermal aging. In contrast, Au/SiO_2/TiO_2 prepared by the deposition-precipitation of gold complex onto SiO_2-doped TiO_2 was not active for CO oxidation. The drastic difference in catalytic performance as a result of different synthesis sequence highlights the importance of rational catalyst design. Further research on the influence of synthesis conditions (e.g., synthesis temperature and Si content) and on the characterization of structural details is warranted.

Acknowledgments

This work was supported by the Office of Basic Energy Sciences, U.S. Department of Energy. The Oak Ridge National Laboratory is managed by UT-Battelle, LLC for the U.S. DOE under Contract DE-AC05–00OR22725. This research was supported in part by the appointment for H.G. Zhu and Z. Ma to the ORNL Research Associates Program, administered jointly by

ORNL and the Oak Ridge Associated Universities. Helpful assistance of Dr. Chengdu Liang in preliminary TEM survey is appreciated.

References

[1] G.A. Somorjai and Y.G. Borodko, Catal. Lett. 76 (2001) 1.
[2] J.M. Thomas and R. Raja, Annu. Rev. Mater. Res. 35 (2005) 315.
[3] F.-S. Xiao, Y. Han, Y. Yu, X.J. Meng, M. Yang and S. Wu, J. Am. Chem. Soc. 124 (2002) 888.
[4] P. Collier, S. Golunski, C. Malde, J. Breen and R. Burch, J. Am. Chem. Soc. 125 (2003) 12414.
[5] Y.G. Tang and R.R. Xu, Top. Catal. 35 (2005) 1.
[6] M. Haruta and M. Daté, Appl. Catal. A 222 (2001) 427.
[7] T.V. Choudhary and D.W. Goodman, Top. Catal. 21 (2002) 25.
[8] H.H. Kung, M.C. Kung and C.K. Costello, J. Catal. 216 (2003) 425.
[9] A.S.K. Hashmi and G.J. Hutchings, Angew. Chem. Int. Ed. 45 (2006) 7896.
[10] G.C. Bond, Louis C. and D.T. Thompson, *Catalysis by Gold*, (Imperial College Press, London, 2006).
[11] G. Pattrick, E. van der Lingen, C.W. Corti, R.J. Holliday and D.T. Thompson, Top. Catal. 30(31) (2004) 273.
[12] W.F. Yan, S.M. Mahurin, S.H. Overbury and S. Dai, Top. Catal. 39 (2006) 199.
[13] W.F. Yan, B. Chen, S.M. Mahurin, E.W. Hagaman, S. Dai and S.H. Overbury, J. Phys. Chem. B 108 (2004) 2793.
[14] W.F. Yan, S.M. Mahurin, B. Chen, S.H. Overbury and S. Dai, J. Phys. Chem. B 109 (2005) 15489.
[15] Y. Tai, J. Murakami, K. Tajiri, F. Ohashi, M. Daté and S. Tsubota, Appl. Catal. A 268 (2004) 183.
[16] A.M. Venezia, F.L. Liotta, G. Pantaleo, A. Beck, A. Horvath, O. Geszti, A. Kocsonya and L. Guczi, Appl. Catal. A 310 (2006) 114.
[17] M.A.P. Dekkers, M.J. Lippits and B.E. Nieuwenhuys, Catal. Today 54 (1999) 381.
[18] X.Y. Xu, J.J. Li, Z.P. Hao, W. Zhao and C. Hu, Mater. Res. Bull. 41 (2006) 406.
[19] K. Qian, W.X. Huang, Z.Q. Jiang and H.X. Sun, J. Catal. 248 (2007) 137.
[20] H.G. Zhu, C.D. Liang, W.F. Yan, S.H. Overbury and S. Dai, J. Phys. Chem. B 110 (2006) 10842.
[21] H.G. Zhu, Z. Ma, J.C. Clark, Z.W. Pan, S.H. Overbury and S. Dai, Appl. Catal. A (2007) in press.
[22] M. Okumura, S. Nakamura, S. Tsubota, T. Nakamura, M. Azuma and M. Haruta, Catal. Lett. 51 (1998) 53.
[23] C.-M. Yang, M. Kalwei, F. Schüth and K.-J. Chao, Appl. Catal. A 254 (2003) 289.
[24] Y.-S. Chi, H.-P. Lin and C.-Y. Mou, Appl. Catal. A 284 (2005) 199.
[25] G. Budroni and A. Corma, Angew. Chem. Int. Ed. 45 (2006) 3328.
[26] W.F. Yan, S.M. Mahurin, Z.W. Pan, S.H. Overbury and S. Dai, J. Am. Chem. Soc. 127 (2005) 10480.
[27] R.J.H. Grisel and B.E. Nieuwenhuys, J. Catal. 199 (2001) 48.
[28] A.C. Gluhoi, X. Tang, P. Marginean and B.E. Nieuwenhuys, Top. Catal. 39 (2006) 101.
[29] Z. Ma, S.H. Overbury and S. Dai, J. Mol. Catal. A (2007) in press.
[30] A. Wolf and F. Schüth, Appl. Catal. A 226 (2002) 1.
[31] S.-H. Wu, X.-C. Zheng, S.-R. Wang, D.-Z. Han, W.-P. Huang and S.-M. Zhang, Catal. Lett. 96 (2004) 49.
[32] W.F. Yan, B. Chen, S.M. Mahurin, V. Schwartz, D.R. Mullins, A.R. Lupini, S.J. Pennycook, S. Dai and S.H. Overbury, J. Phys. Chem. B 109 (2005) 10676.
[33] M.B. Cortie, Gold Bull. 37 (2004) 12.
[34] B.K. Min, W.T. Wallace and D.W. Goodman, J. Phys. Chem. B 108 (2004) 14609.
[35] S. Kielbassa, M. Kinne and R.J. Behm, J. Phys. Chem. B 108 (2004) 19184.
[36] S.H. Overbury, V. Schwartz, D.R. Mullins, W.F. Yan and S. Dai, J. Catal. 241 (2006) 56.
[37] Q.Y. Li, Y.F. Chen, D.D. Zeng, W.M. Gao and Z.J. Wu, J. Nanopart. Res. 7 (2005) 295.
[38] A.M. El-Toni, S. Yin and T. Sato, J. Colloid Interf. Sci. 300 (2006) 123.
[39] Y.Z. Yuan, K. Asakura, H.L. Wan, K. Tsai and Y. Iwasawa, Catal. Lett. 42 (1996) 15.
[40] G. Martra, L. Prati, C. Manfredotti, S. Biella, M. Rossi and S. Coluccia, J. Phys. Chem. B 107 (2003) 5453.
[41] J. Chou, N.R. Franklin, S.-H. Baeck, T.F. Jaramillo and E.W. McFarland, Catal. Lett. 95 (2004) 107.
[42] Z. Yan, S. Chinta, A.A. Mohamed, J.P. Fackler and D.W. Goodman, Catal. Lett. 111 (2006) 15.
[43] L.D. Menard, F.T. Xu, R.G. Nuzzo and J.C. Yang, J. Catal. 243 (2006) 64.
[44] C.-W. Chiang, A.Q. Wang and C.-Y. Mou, Catal. Today 117 (2006) 220.
[45] M. Comotti, W.C. Li, B. Spliethoff and F. Schüth, J. Am. Chem. Soc. 128 (2006) 917.
[46] X.Z. Fu, W.A. Zeltner, Q. Yang and M.A. Anderson, J. Catal. 168 (1997) 482.
[47] S. Ek, E.I. Iiskola, L. Niinistö, J. Vaittinen, T.T. Pakkanen, J. Keränen and A. Auroux, Langmuir 19 (2003) 10601.
[48] D. Hausmann, J. Becker, S.L. Wang and R.G. Gordon, Science 298 (2002) 402.
[49] S. Poovarodom, J.D. Bass, S.J. Hwang and A. Katz, Langmuir 21 (2005) 12348.
[50] H.F. Yin, W.F. Yan and S. Dai, unpublished results.
[51] X.Y. Deng, Z. Ma, Y.H. Yue and Z. Gao, J. Catal. 204 (2001) 200.
[52] B. Schumacher, V. Plzak, M. Kinne and R.J. Behm, Catal. Lett. 89 (2003) 109.
[53] A. Horváth, A. Beck, A. Sárkány, G. Stefler, Z. Varga, O. Geszti, L. Tóth and L. Guczi, J. Phys. Chem. B 110 (2006) 15417.
[54] L. Guczi, Z. Pászti, K. Frey, A. Beck, G. Pető and C.S. Daróczy, Top. Catal. 39 (2006) 137.
[55] B. Solsona, M. Conte, Y. Cong, A. Carley and G. Hutchings, Chem. Commun. (2005) 2351.
[56] P. Mohapatra, J. Moma, K.M. Parida, W.A. Jordaan and M.S. Scurrell, Chem. Commun. (2007) 1044.
[57] Z. Ma, S. Brown, S.H. Overbury and S. Dai, Appl. Catal. A (2007) submitted.
[58] F. Wang and G. Lu, Catal. Lett. 115 (2007) 46.
[59] T. Kanazawa, Catal. Lett. 108 (2006) 45.
[60] S. Mahurin, L.L. Bao, W.F. Yan, C.D. Liang and S. Dai, J. Non-Cryst. Solids 352 (2006) 3280.
[61] Z. Ma, F. Zaera, in: *Encyclopedia of Inorganic Chemistry*, eds. R.B. King, (Second Edition), (Chichester, 2005) pp. 1768.
[62] L. Gamble, M.A. Henderson and C.T. Campbell, J. Phys. Chem. B 102 (1998) 4536.
[63] Z. Ma and F. Zaera, Surf. Sci. Rep. 61 (2006) 229.